THE GERONTOLOGICAL SOCIETY OF AMERICA®

Journals of Gerontology: Biological Sciences
cite as: *J Gerontol A Biol Sci Med Sci*, 2020, Vol. 75, No. 1, 89–98
doi:10.1093/gerona/glz177
Advance Access publication July 29, 2019

OXFORD

Translational Section: Drug Interventions

Original Article

Life-span Extension Drug Interventions Affect Adipose Tissue Inflammation in Aging

Theresa Mau, PhD,[1,2] Martin O'Brien, BS,[1] Amiya K. Ghosh, PhD,[1] Richard A. Miller, PhD,[3] and Raymond Yung, MB, ChB[1–4,*]

[1]Division of Geriatric and Palliative Medicine, Department of Internal Medicine, [2]Graduate Program in Immunology, Program in Biomedical Sciences (PIBS), and [3]Department of Pathology and Glenn Center for Biology of Aging Research, University of Michigan, Ann Arbor. [4]Geriatric Research, Education, and Clinical Care Center (GRECC), VA Ann Arbor Health System, Michigan.

*Address correspondence to: Raymond Yung, MB, ChB, Division of Geriatric and Palliative Medicine, Department of Internal Medicine, University of Michigan, Ann Arbor, MI 48109. E-mail: ryung@umich.edu

Received: March 11, 2019; Editorial Decision Date: July 21, 2019

Decision Editor: David Le Couteur, MBBS, FRACP, PhD

Abstract

The National Institute on Aging (NIA)-sponsored Interventions Testing Program (ITP) has identified a number of dietary drug interventions that significantly extend life span, including rapamycin, acarbose, and 17-α estradiol. However, these drugs have diverse downstream targets, and their effects on age-associated organ-specific changes are unclear (Nadon NL, Strong R, Miller RA, Harrison DE. NIA Interventions Testing Program: investigating putative aging intervention agents in a genetically heterogeneous mouse model. *EBioMedicine*. 2017;21:3–4. doi:10.1016/j.ebiom.2016.11.038). Potential mechanisms by which these drugs extend life could be through their effect on inflammatory processes often noted in tissues of aging mice and humans. Our study focuses on the effects of three drugs in the ITP on inflammation in gonadal white adipose tissue (gWAT) of HET3 mice—including adiposity, adipose tissue macrophage (ATM) M1/M2 polarization, markers of cellular senescence, and endoplasmic reticulum stress. We found that rapamycin led to a 56% increase of $CD45^+$ leukocytes in gWAT, where the majority of these are ATMs. Interestingly, rapamycin led to a 217% and 106% increase of M1 ($CD45^+CD64^+CD206^-$) ATMs in females and males, respectively. Our data suggest rapamycin may achieve life-span extension in part through adipose tissue inflammation. Additionally, HET3 mice exhibit a spectrum of age-associated changes in the gWAT, but acarbose and 17-α estradiol do not strongly alter these phenotypes—suggesting that acarbose and 17- α estradiol may not influence life span through mechanisms involving adipose tissue inflammation.

Keywords: ITP, Life span, Aging, Adipose tissue, Macrophage

Human aging is, in part, characterized by the tendency of the body to develop a proinflammatory status with advancing age (1–7). Chronic inflammation plays an important role in the pathogenesis of many age-associated diseases (8–10), such as Alzheimer's disease, atherosclerosis, cardiovascular disease, type II diabetes, and invasive cancer. Adipose tissue inflammation is believed to be a major contributor to a range of age-related functional declines (11–13). Effects of abnormalities in adipose tissue could in principle be mediated by changes in energy storage, lipid metabolism, or production and secretion of adipokines and hormones.

With advancing age in humans and rodents, adipose tissue mass increases through middle and early-old age, and white adipose tissue (WAT) redistributes from subcutaneous to intra-abdominal visceral depots (14–18). WAT also exhibits ectopic lipid infiltration in liver, muscle, and bone (17–19)—though rodent models of lipodystrophy are still being developed and lack data from females (20–22). In gonadal WAT (gWAT), the distribution of adipose tissue macrophage (ATM) subsets shift toward proinflammatory phenotypes with age (23–25). We have previously shown that in gWAT of old (22 months) C57BL/6J male mice, ATMs shifted from an anti-inflammatory "M2" phenotype ($CD206^+$) to the

proinflammatory "M1" ($CD206^-$) phenotype when compared to young (6 months) controls (23). This upward shift in M1:M2 ATMs ratio was associated with increased levels of proinflammatory chemokines and cytokines, including monocyte chemoattractant protein-1 (MCP-1), tumor necrosis factor alpha (TNFα), and interleukin-6 (IL-6). Although the M1/M2 distinction over-simplifies a network of interrelated cell types of overlapping function, we will, for the purpose of discussion, refer to $CD45^+CD64^+CD206^-$ macrophages as "M1s" and $CD45^+CD64^+CD206^+$ macrophages as "M2s" in this report.

Our subsequent studies revealed that endoplasmic reticulum (ER) stress plays a significant role in ATM inflammation in aging-associated obesity. Alleviation of ER stress in old murine-derived ATMs blocked secretion of IL-6, TNF-α, and MCP-1, restoring a phenotype to that of young ATMs (25,26). Another notable source of inflammation in aging adipose tissue is production of inflammatory cytokines by senescent cells, termed senescence-associated secretory phenotype (SASP). Relative to other tissues (brain, liver, colon, lung, pancreas, and heart), WAT, along with skeletal muscle and the eyes, is a major reservoir for $p16^{Ink4a}$ and senescence-associated β-galactosidase (SA-β-Gal) senescent cell accumulation. There is some evidence that reduction of $p16^{Ink4a}$ senescent cells may attenuate the onset of age-related disorders, at least in a mouse model of progeria (27,28). However, the inflammatory status of the specific aging tissues that seem to benefit from the senolytics were unexplored—necessitating future work to question whether or not the reduction of senescent cells directly diminishes adipose tissue inflammation.

These changes in aging adipose tissue collectively contribute to age-associated adipose tissue dysfunction, which affects health and life span (29). Interventions for life-span extension target nutrient-sensing pathways that also have significant effects on adipose tissue in lower organisms (30–34). In a few cases, mutations that extend life span in lower organisms, such as flies or worms, also lead to life-span extension when the mutation is limited to adipose tissue (35,36). Fat-specific insulin receptor knockout (FIRKO) mice have reduced fat mass, protection from age-associated obesity, and mean life span extended by 18% (32). In the current study, we hypothesized that Interventions Testing Program (ITP) pharmacological interventions, specifically acarbose (ACA), 17-α estradiol (17aE2), and rapamycin (Rapa), may extend life by slowing or preventing age-related increases in adipose tissue inflammation. We measure aspects of adipose tissue composition and function in six groups of HET3 mice (young, old, calorie restriction [CR], ACA, 17aE2, and Rapa), with emphasis on the levels of adipose tissue ER stress and the relative proportions of ATM subsets. Additionally, we evaluate the effects of age on HET3 mouse adipose tissue and whether any of the ITP drugs influence these age-related phenotypes.

Previous studies (37–43) of the ITP drugs have reported on the sex differences, extent of life-span extension, and dose-dependent response using genetically heterogeneous HET3 mice. In this system, 30% caloric or dietary restriction can extend life in female and male mice by 36% (44). ACA, which blunts post-prandial glucose spikes, extends male life span by 22% and leads to an increase of only 5% in females (42). 17aE2 does not extend life span of females but extends male life span by 19% (42). Rapa, which inhibits the mechanistic target of rapamycin (mTOR) kinase, can extend life span in females by 26% and in males by 23% at the highest doses tested (37,38,40,45). Further details on the National Institute on Aging (NIA) ITP (https://www.nia.nih.gov/research/dab/interventions-testing-program-itp) are summarized (46).

Materials and Methods

Animals: Breeding and Husbandry Protocol

Genetically heterogeneous UM-HET3 mice were produced via a four-way cross between CbyB6F1/J mothers (BALB/cByJ × C57BL/6J, JAX #100009) and C3D2F1/J fathers (C3H/J × DBA/2J, JAX #100004) at University of Michigan (UM) as previously described (47). The mice were housed in pairs per cage from weaning, cages were inspected daily, and mice that died were not replaced. At 4 months of age, F1 mice from different breeding pairs were randomly allocated among five groups: controls, CR, Aca, 17aE2, and Rapa treatment groups. These mice were euthanized at age 22 months, along with a comparison group of young (4 months) animals of both sexes.

Control and Experimental Diets

Breeding pairs were fed Purina 5008 chow. Young (4 months) and old (22 months) control mice were fed the Purina 5LG6 chow starting at weaning. Control and treatment diets were prepared by TestDiet, Inc., Purina Mills (Richmond, IN). For CR, mice 4 months of age were given an amount of food equal to 90% of the amount consumed by mice in the control group for 2 weeks, then limited to 75% for 2 weeks and then limited to 60% for the remainder of the experiment (48). ACA was purchased from Spectrum Chemical Mfg. Corp. (Gardena, CA), and given to the mice at 1,000 ppm (ie, 0.1% by weight of food) from 4 months of age. 17aE2 was purchased from Steraloids Inc. (Newport, RI) and provided to mice at 14 ppm from 9 months of age. Encapsulated Rapa was provided from 4 months of age at 14.7 ppm.

Tissue Extraction: gWAT Stromal Vascular Fraction

gWAT is removed with minimal cuts, weighed, and placed into a sterile petri dish containing ice cold dye-free Dulbecco's modified Eagle medium (DMEM) containing 10% fetal bovine serum (FBS) (Gibco 21063-029) and 1% penicillin–streptomycin (Gibco 15140-122). Collagenase (Sigma Life Science, #C6885-1G) is prepared in DMEM buffer with a final 10 mg/mL concentration. gWAT fat pads were minced, gently passed through 100-μm filter, centrifuged (1,500 rpm), and collagenase-digested in an 37 °C incubator for 45 minutes with rotation. A second rinse-filter step follows. ACK lysis (Lonza, #10-548E) is mixed into cell pellets and neutralized at 5 minutes with ice cold phosphate-buffered saline (PBS). A third rinse-filter step occurs with cold PBS. Stromal vascular fraction (SVF) cells are resuspended in 1 mL of cold PBS and 10 μL is saved for trypan blue (Invitrogen) cell counting using the Cell Countess (Invitrogen).

Flow Cytometry Stains

SVF cells extracted from gWAT are washed and resuspended in sterile filtered fluorescence-activated cell sorting (FACs) buffer (PBS, 0.5% bovine serum albumin [BSA], 0.1% NaN_3) and cells per sample are pooled together to form the control cells for single positive controls (SPCs), Full-minus-one Controls (FMOs), and the negative cells. Samples are blocked with anti-mouse CD16/CD32 (eBioscienceaffymetrix #14-0161) for 1 hour on ice. After rinsing, cells are incubated with anti-mouse CD45 (eBioscienceaffymetrix #48-0451), CD64 (BD Pharmingen 558455), CD11c (eBioscienceaffymetrix #47-0114), CD11b (eBioscienceaffymetrix #11-0112), CD206 (eBioscienceaffymetrix #17-2061), and CD31 (eBioscienceaffymetrix #46-0311) for 1 hour on ice, in foil. Cells were fixed with 2% paraformaldehyde (PFA) for 20 minutes on ice prior to washing and storing in FACs buffer until analysis. Samples were run on a LSRFortessa (University of Michigan Flow Cytometry Core) and analyzed on FlowJo version 10.0.0.1.

mRNA Isolation and RT–qPCR

Total RNA was isolated from whole gWAT and inguinal WAT (iWAT), homogenized in Qiazol lysis reagent (Qiagen, #1023537), and processed through a QIAshredder (Qiagen, #79656) prior

to using the RNeasy Lipid Tissue Mini Kit (Qiagen, #1023539) in conjunction with a RNase-Free DNase (Qiagen, #79254) digestion step. Reverse transcription and cDNA amplification were performed with QuantiTect SYBR Green RT-PCR Kit (Qiagen, #1054498) on a real-time R6-6006 Corbett Thermalcycler in duplicates, and each sample is normalized to the average expression of its *Gapdh*. All primers were obtained from Integrated DNA Technologies (IDT) and specific primer sequences are listed (Supplementary Table 1).

Statistical Analyses

Two-way analysis of variance (ANOVA) analyses were performed, setting factor 1 = sex [female; male], factor 2 = old controls and one other group [young controls, CR-, ACA-, 17aE2-, or Rapa-treated mice]. Interaction term = Sex term × Treatment term, each reported (*p < .05, **p < .01, ***p < .001, ****p < .0001). A post hoc test used as a follow-up was Sidak's multiple comparisons, reporting average difference in mean for each sex (*p < .05, **p < .01, ***p < .001, ****p < .0001). If interaction or sex effect were insignificant, sexes were pooled and submitted to normality tests D'Agostino and Pearson and Shapiro–Wilks (α = .05). If normality test passes ($p \geq .05$), then a Student's unpaired *T*-test (abbreviated as "T" in Supplementary Table 3) is run and if significant (^p < .05, ^^p < .01, ^^^p < .001, ^^^^p < .0001), degree of significance and average difference in mean were reported. If normality test fails ($p \leq .05$), then a Mann–Whitney (abbreviated as "MW" in Supplementary Table 3) test is run, and if significant ($^{\#}p$ < .05, $^{\#\#}p$ < .01, $^{\#\#\#}p$ < .001, $^{\#\#\#\#}p$ < .0001), degree of significance and average difference in median were reported.

Results

Genetically heterogeneous HET3 mice were assigned to either young or old controls. CR, ACA, 17aE2, and Rapa treatment began at 4 months of age with the exception of 17aE2 mice which were placed on 17aE2 treatment diet at 9 months of age (Figure 1A). Values reported within text are mean ± SEM. Supplementary Table 2 contains a concise summary of statistically significant findings. Where there are significant sex effects, percent change is reported within the text. Occasionally, the follow-up Sidak's comparisons test (for individual sexes) does not reach statistical significance, and these cases are denoted as not significant (N.S.) (Supplementary Table 3). These trends may be reported to highlight the sex effects and will be further explored in discussion. *P*-values reported for interaction (Sex × Treatment), sex, or treatment represent two-way ANOVA results and are comprehensively reported in Supplementary Table 3, with further details on this table within the statistical methods section. In cases where the sex and/or interaction term in the two-way ANOVA is insignificant, the mean ± SEM reported represent data pooled across sexes.

Life-span Extension Drugs and Adiposity

With age, the changes in rodent and human adipose tissue distribution and mass lead to an age-associated form of obesity (12,16–18). HET3 mice steadily gain weight through middle age, and often undergo age-related weight decline beginning at approximately 18 months of age (40,45). Similar to reports in human aging (16,17,49), advanced stages of aging in HET3 mice are characterized by a decline in body weight, and this was clearly present in males and to a lesser extent in females (42). In this current study, we report

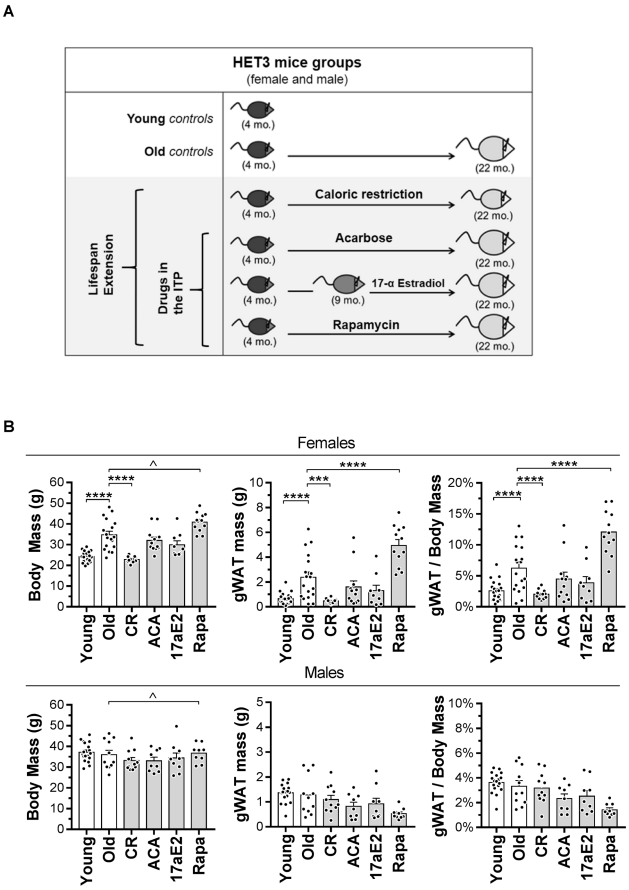

Figure 1. Interventions Testing Program (ITP) drug interventions differentially influence gonadal white adipose tissue (gWAT) and body mass ratio of HET3 mice. (**A**) HET3 mice in drug-intervention timeline. All mice were analyzed at 22 months of age except for young controls which were 4 months of age. (**B**) Total body mass and gWAT mass (one fat pad per mouse) were measured, and gWAT-to-body mass ratios were calculated. n = 9–19 per group of mice. Error bars are SEM. Two-way analysis of variance (ANOVA), Sidak's multiple comparison's post hoc test (*p < .05, **p < .01, ***p < .001, ****p < .0001). If no sex effect was significant, sexes were pooled for analyses with either Student's unpaired *T*-test (^p < .05, ^^p < .01, ^^^ p < .001, ^^^^p < .0001) or by Mann–Whitney if normality tests failed ($^{\#}p$ < .05, $^{\#\#}p$ < .01, $^{\#\#\#}p$ < .001, $^{\#\#\#\#}p$ < .0001).

HET3 mice weights at 22 months of age, a time point that likely reflects, on average, a 4-month period of age-related decline in body mass. Consistent with previous studies, old control females (34.7 ± 1.71 g) weigh more than young control females (24.1 ± 0.6 g; p < .001), while there are no significant differences in average body mass between old (36.0 ± 2.1 g) and young (37.1 ± 1.1 g) control males (Figure 1B).

In CR mice, interaction between sex and treatment on body mass is significant (p < .01). Old CR females have body masses (22.9 ± 0.4 g) similar to their young counterparts and weigh less than old control females (34.7 ± 1.7 g; p < .0001) (Figure 1B). The age-associated loss of fat in old control males (36.0 ± 2.1 g) may be why these mice are statistically indistinct from old CR males (33.2 ± 1.5 g) in body mass. Consistent with our previous study (42), 17aE2-treated HET3 mice of both sexes have no significant body mass differences at 22 months of age. ACA-treated mice also do not have changes to body mass when compared to old controls. However, we have previously observed that ACA-treated females

developed smaller body masses than old control females (42), and therefore interpretation of this data should take this into account. In another study, when Rapa treatment was administered beginning at 9 months of age, we observed trends of smaller body weights at the highest dosage (42 ppm), while moderate dosage (14 ppm) induced no significant body weight changes in either sex (40). In this current study, we observe that when Rapa treatment is initiated at 4 months of age at the moderate dosage, body mass of Rapa-treated female and male mice (39.1 ± 1.1 g) is significantly higher than old controls (35.2 ± 1.3 g; $p < .05$) when evaluated at 22 months.

We next compared the masses of gWAT from each mouse (Figure 1B). The interaction between age and gender is significant for gWAT mass ($p < .01$), indicating that at 22 months, gWAT fat pads are different between the two sexes. Consistent with reported aging trends on visceral fat mass gain in humans (17,18) and rodents (14,50), old female mice (2.4 ± 0.4 g) have larger gWAT pads than young females (0.7 ± 0.1 g; $p < .0001$). We observe no significant mass difference between young (1.4 ± 0.1 g) and old (1.3 ± 0.2 g) male fat pads. Without gWAT measurements at 12 and 18 months of age, we are unable to conclude whether the age trajectory of gWATs mass in males differs from that in females or if their age-related decline in total body weight heavily stems from gWAT mass loss. There is a significant interaction between sex and CR in gWAT mass ($p < .05$). CR female mice (0.5 ± 0.1 g) develop smaller fat pads than old non-CR females (2.4 ± 0.4 g; $p < .0001$), shifting them toward sizes similar to young females (0.7 ± 0.1 g). ACA- and 17aE2-treated mice have a modest decline in fat pad sizes that did not reach statistical significance (Supplementary Figure 1). In contrast, Rapa-treated female mice (5.0 ± 0.5 g) have a substantial increase in their fat pad masses compared to controls (2.4 ± 0.4 g; $p < .001$), while Rapa-treated male mice (0.5 ± 0.1 g) are on average lower than controls (1.3 ± 0.2 g, N.S.). Given this difference, interaction between sex and Rapa treatment is highly significant ($p < .0001$).

To account for body mass differences, we also calculated the fat pad to body mass ratio for each mouse (Figure 1B). In congruence with the fat pad and body mass analysis, this ratio is significantly increased between young (2.6 ± 0.4%) and old (6.2 ± 0.9%; $p < .0001$) females but not between young (3.6 ± 0.2%) and old (3.3 ± 0.5%) males. CR treatment in female mice (2.0 ± 0.2%) leads to smaller fat pad to body ratio than controls (6.2 ± 0.9%; $p < .001$), and ITP drugs ACA and 17aE2 do not affect either sex. In contrast, Rapa-treated female mice (12.1 ± 1.0%) have an increase to their gWAT-to-body mass ratio compared to controls (6.2 ± 0.9%; $p < .0001$). This indicates that Rapa treatment in females shifts gWAT mass away from a younger phenotype and leads to gonadal fat pad expansion well beyond the age-related fat mass gain observed in old female controls. Interestingly, while Rapa-treated female mice have a ~95% increase in gWAT-to-body mass ratio, Rapa-treated male mice (1.4 ± 0.2%) have a ~58% decrease from old control males' gWAT-to-body mass ratio (3.3 ± 0.5%, N.S.).

SVF Density in gWAT Is Altered by Certain ITP Drugs

To study the immune composition of the gWAT, we first separated the SVF cells of the gWAT from the adipocyte fraction. We have previously reported an increase in gWAT SVF cells in old C57BL/6J males (22 months) compared to young males (6 months) (23). Here, using HET3 mice, we observe a significant effect of age in the gWAT SVF cell numbers in females ($p < .05$). Old females ($4.0 \times 10^6 \pm 0.6 \times 10^6$ cells) have significantly higher total SVF count than young females ($1.3 \times 10^6 \pm 0.4 \times 10^6$ cells; $p < .001$) (Figure 2A). CR mice ($1.4 \times 10^6 \pm 0.1 \times 10^6$ cells) and 17aE2-treated mice ($1.6 \times 10^6 \pm 0.4 \times 10^6$ cells) have lower SVF count than old controls ($4.0 \times 10^6 \pm 0.5 \times 10^6$ cells; CR: $p < .0001$, 17aE2: $p < .001$). Rapa treatment significantly increases total SVF in both sexes ($6.6 \times 10^6 \pm 1.0 \times 10^6$ cells; $p < .05$) (Figure 2A). Interestingly, CR- and 17aE2-treated mice have trends of shifting the SVF count down while Rapa treatment appears to increase these cells in both sexes.

To ask whether the density of SVF cells changes with age or ITP drug treatment, we normalized the total SVF cells per gram of gWAT mass in individual mice (Figure 2A). The density of gWAT SVF cells is sex- and age-dependent (interaction, $p < .05$). Old females ($1.6 \times 10^6 \pm 0.1 \times 10^6$ cells/g gWAT) have a significant decrease of gWAT SVF cell density compared to young females ($2.9 \times 10^6 \pm 0.4 \times 10^6$

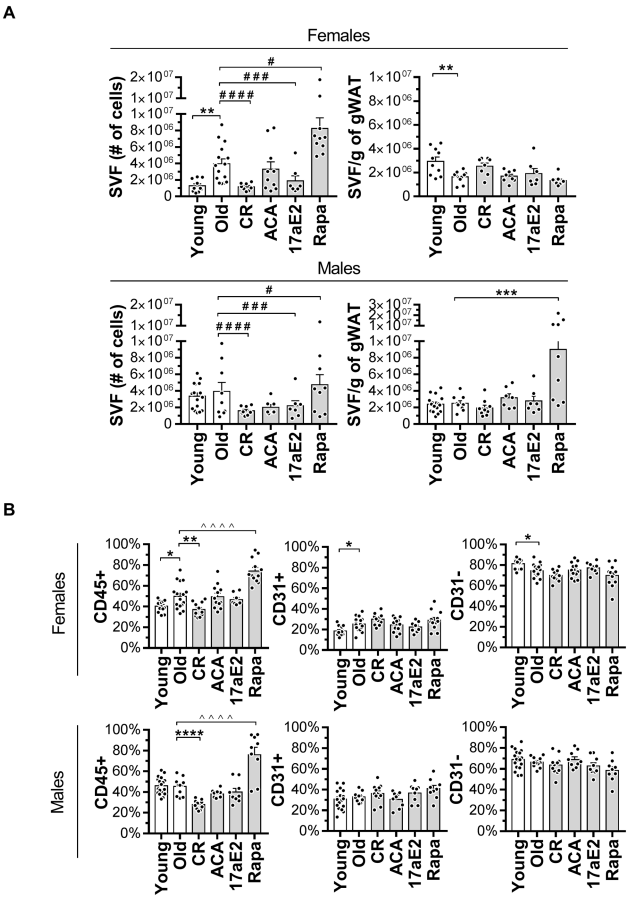

Figure 2. Calorie restriction (CR) and rapamycin alter gonadal white adipose tissue (gWAT) cell density and CD45⁺ leukocyte frequencies differently. (**A**) Stromal vascular fraction (SVF) total cell numbers are reported for each mouse, separated by sex. n = 9–19 per group of mice. On the right, SVF cell counts are normalized to each mouse's gWAT mass which provides a cell density value as number of cells per 1 g of gWAT. (**B**) Flow cytometry of gWAT leukocytes, endothelial cells, and cells enriched for adipose tissue stem cells (ATSCs). n = 9–19 per group of mice. CD45⁺ leukocyte frequency is reported as % singlets, and CD31⁺ endothelial cells and CD31⁻ ATSC-enriched cells are reported as % CD45⁻ cells. Error bars are SEM. Two-way analysis of variance (ANOVA), Sidak's multiple comparison's post hoc test (*$p < .05$, **$p < .01$, ***$p < .001$, ****$p < .0001$). If no sex effect was significant, sexes were pooled for analyses with either Student's unpaired T-test (^$p < .05$, ^^$p < .01$, ^^^$p < .001$, ^^^^$p < .0001$) or by Mann–Whitney if normality test failed (#$p < .05$, ##$p < .01$, ###$p < .001$, ####$p < .0001$).

cells/g gWAT; $p < .01$). CR and ITP drugs ACA and 17aE2 do not alter SVF density. Rapa-treated males ($4.8 \times 10^6 \pm 1.2 \times 10^6$ cells/g gWAT) have significantly increased SVF density compared to control males ($3.9 \times 10^6 \pm 1.1 \times 10^6$ cells/g gWAT; $p < .001$).

gWAT SVF Immune Compartment

The gWAT SVF cells that remain after collagenase digestion contain preadipocytes, endothelial cells, immune cells, and other non-fat cells (23,51). In humans and rodents, there is some evidence supporting the notion that SVF produces more proinflammatory mediators than adipocytes (23), which are known to also secrete adipokines and also contribute to inflammation (51). In this study, we observe an increase of $CD45^+$ leukocytes in the gWAT of old females (49.8 ± 3.0%) compared to young females (40.4 ± 1.7%; $p < .05$), and no changes were noted between old (45.4 ± 2.5%) and young (46.1 ± 2.0%) males (Figure 2B). CR affects leukocyte frequency in a sex-dependent manner ($p < .05$) and leads to 26% and 38% decreased leukocyte frequencies in females (37.1 ± 2.0%; $p < .01$) and males (28.0 ± 1.3%; $p < .0001$) respectively. ACA and 17aE2 do not alter leukocyte frequencies in either sex. When compared to old control mice (48.1 ± 2.1%), Rapa-treated mice of both sexes have a substantial increase in $CD45^+$ leukocytes (75.1 ± 3.5%; $p < .0001$). We next analyze $CD45^-CD31^+$ endothelial cell numbers and find no overall differences, although old females (25.3 ± 1.6%) have a modest increase compared to young cohorts (18.4 ± 1.4%; $p < .05$). $CD45^-CD31^-$ cells are analyzed as cells enriched for adipose tissue stem cells (ATSCs), but it appears none of the ITP drugs alter this compartment significantly.

Adipose Tissue Macrophages

ATMs play a considerable role in adipose tissue inflammation (23). Many studies of ATMs in mice have used CD11b and F4/80, and both of these markers also identify subsets of dendritic cells (DCs) and eosinophils. In an effort to disentangle these overlaps, the Immunological Genome Project identified a core murine macrophage marker, FcγR1 (CD64) (52). It has been shown that the $CD45^+CD64^+$ combination is specific for ATMs not only in C57BL/6J male mice gWAT but also in human omental and subcutaneous adipose tissues (53). In our data, there is no effect of aging on $CD45^+CD64^+$ ATM frequencies in either sex (Figure 3)—similar to what we have previously reported in young (6 months) and old (22 months) C57BL/6J male mice (23). CR mice of both sexes (51.0 ± 1.9%) have a significant increase in ATM frequency compared to controls (40.5 ± 2.4%; $p < .01$). Neither ACA nor 17aE2 alters the frequency of total ATMs. There is a sex difference with Rapa treatment effects on total ATM frequency ($p < .05$). Rapa-treated females (51.4 ± 4.4%) have a 33% increase in ATM frequency compared to old females (38.6 ± 3.2%; $p < .05$), whereas Rapa-treated males (67.3 ± 4.3%) have a 55% increase compared to old males (43.5 ± 3.8%; $p < .001$). Rapa significantly increases the proportion of $CD64^+$ cells sufficient to account for the increase in total $CD45^+$ cells in mice treated with this drug (Figure 3A; Supplementary Figure 1A). We observe a sex- and age-dependent (interaction $p < .05$) decrease of $CD45^+CD64^-CD11c^+$ DCs in old males (14.9 ± 0.6%) compared to young males (28.6 ± 2.9%; $p < .0001$) (Figure 3B). Of the three ITP drugs we tested, only Rapa (6.4 ± 1.3%) alters these DCs in males, shrinking this population by 57% when compared with old controls ($p < .001$).

In aged mice, ATMs shift toward M1-polarized "proinflammatory" macrophages, away from M2-polarized "anti-inflammatory" macrophages (23). We observe a significant sex difference in the age-associated

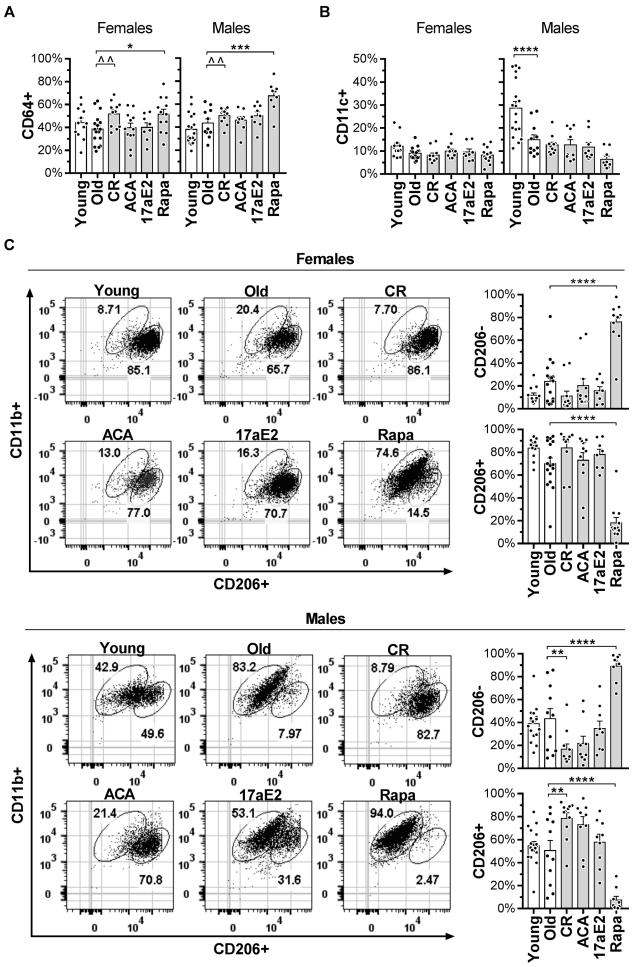

Figure 3. Life-span extension drugs affect adipose tissue macrophage polarization. Flow cytometry of gonadal white adipose tissue (gWAT). (**A**) $CD64^+$ macrophages reported as % $CD45^+$ cells and (**B**) $CD11c^+$ dendritic cells reported as % $CD45^+CD64^-$ cells. $n = 9$–19 per group and sex. (**C**) Representative flow panel, $n = 2$ per group and sex. Gates: (y-axis) singlets > $CD45^+$ > $CD64^+$ > $CD11b^+$ and $CD206^+$ (x-axis). "M1" ($CD206^-$) and "M2" ($CD206^+$) macrophages reported as % $CD45^+CD64^+CD11b^+$ cells. Error bars are SEM. Two-way analysis of variance (ANOVA), Sidak's multiple comparison's post hoc test (*$p < .05$, **$p < .01$, ***$p < .001$, ****$p < .0001$). If no sex effect was significant, sexes were pooled for analyses with either Student's unpaired *T*-test (^$p < .05$, ^^$p < .01$, ^^^$p < .001$, ^^^^$p < .0001$) or by Mann–Whitney if normality test failed ($^{\#}p < .05$, $^{\#\#}p < .01$, $^{\#\#\#}p < .001$, $^{\#\#\#\#}p < .0001$).

ATM phenotypic switch in HET3 mice (Figure 3C; Supplementary Table 3). These sex effects are present in both $CD45^+CD64^+CD206^-$ "M1" ATM frequencies ($p < .0001$) and $CD45^+CD64^+CD206^+$ "M2" ATM frequencies ($p < .0001$). CR yields significant and modest sex effects on M1 and M2 ATM frequencies ($p < .05$ and $p < .05$) as well.

M1 Adipose Tissue Macrophages

Old females (24.0 ± 4.8%) have a 103% increase in M1 ATMs compared to young females (11.8 ± 2.1%, N.S.), and old males (43.4 ± 8.8%) have an 11% increase of M1 ATMs compared to young males (39.0 ± 3.5%, N.S.) (Figure 3C). M1 ATMs in CR females (11.2 ± 4.2%) decreases by 53% compared to old females (N.S.), and CR male mice (16.7 ± 4.5%) have a 62% decrease in M1 ATMs compared to old males ($p < .01$). ACA- and 17aE2-treated mice have M1/M2 shifts similar to CR, though Sidak's multiple comparisons do

not identify any significant drug effects in either sex (Supplementary Table 3). In contrast, Rapa treatment leads to substantial increases to M1 macrophages in both sexes (Figure 3C) and modest sex differences in M1/M2 ATMs ($p < .05$; Supplementary Table 3). Rapa-treated females (76.1 ± 5.3%) have a 217% increase of M1-polarized ATMs compared to old controls ($p < .0001$), and similarly, but to a lesser extent, Rapa-treated males (89.2 ± 3.9%) have a 106% increase in their M1 ATM population ($p < .0001$).

M2 Adipose Tissue Macrophages

Naturally, the shifts in M1 polarization ($CD206^-$ ATMs) are accompanied by a proportional switch in M2 polarization ($CD206^+$ ATMs) in these mice (Figure 3C). Old females (70.0 ± 5.0%) have a 17% decrease of M2 ATMs compared to young females (83.8 ± 2.5%; N.S.), whereas old males (50.5 ± 8.8%) have an 8% decrease of M2 ATMs compared to young males (54.7 ± 3.6%; N.S.). CR increases M2 ATMs 20% compared to old females (83.8 ± 5.3%; N.S.) and 55% M2 ATMs compared to old males (78.4 ± 5.0%; $p < .01$). Compared to old controls, Rapa-treated females (18.1 ± 4.6%) have a 74% decrease of M2-polarized ATMs ($p < .0001$), and Rapa-treated males (7.5 ± 3.2%) have an 85% decrease to their M1 ATM population ($p < .0001$). In addition, Rapa-treated mice have a 24% and 37% decrease in frequency of non-macrophage and non-DC leukocytes (T and B lymphocytes, eosinophils, etc.) that were $CD45^+CD64^-CD11c^-$ in females ($p < .05$) and males ($p < .05$), respectively (Supplementary Figure 1B).

ER stress responses in gWAT contribute to adipose tissue inflammation in aging. To determine if ITP drugs modify adipose tissue ER stress, we evaluated mRNA for *Bip*, *Atf4*, and *Chop* (Figure 4A). Old control mice of both sexes (1.8 ± 0.4 AU) have increased *Chop* compared to young controls (1.2 ± 0.3 AU; $p < .01$). CR improves ER stress responses in old HET3 mice: *Chop* is significantly reduced in both sexes (0.7 ± 0.1 AU; $p < .0001$). CR mice of both sexes (1.1 ± 0.1 AU) also have significantly decreased *Atf4* compared to old controls (2.2 ± 0.2 AU; $p < .001$). ITP drugs ACA and 17aE2 do not appear to affect life-span extension through ER stress in the adipose tissue. Whereas, Rapa-treated females (3.5 ± 0.5 AU) have an increase in *Bip* compared to old females (2.3 ± 0.5 AU; $p < .05$), and Rapa-treated mice (3.2 ± 0.5 AU) also have an increase in *Atf4* compared to old controls ($p < .05$). Overall, we conclude that ITP drugs we tested do not alter ER stress in gWAT, with the possible exception of Rapa treatment.

It has been postulated that age-related declines in browning and beiging adipose tissue activity in humans (54) and rodents (55,56) are contributing factors to age-related adiposity. To test if (i) old HET3 mice have an effect of age on gWAT thermogenic factors and whether or not (ii) any ITP drugs modulated them, we measured mRNA of beige or "brite" (browning of WAT) markers in unstimulated whole gWAT normalized to *Gapdh* mRNA (Figure 4B). We measure thermoregulatory factors that both brown and beige adipocytes express mitochondrial uncoupling protein 1 (*Ucp1*) and brown fat cell-enriched protein *Cidea*. We also measure *CD137*, a beige-selective marker (56) and zinc finger protein PR domain containing 16 (*Prdm16*) which is crucial for browning of WAT (57). CR leads to decreased *CD137* in both females and males (0.7 ± 0.1 AU) compared to old controls (1.7 ± 0.3 AU; $p < .001$). Rapa leads to increased *CD137* expression (Rapa: 2.8 ± 0.3 AU, old: 1.7 ± 0.3 AU; $p < .05$). Old females (1.9 ± 0.3 AU) have higher *Prdm16* than young females (0.9 ± 0.1 AU; $p < .01$), and old males (3.0 ± 0.6 AU) also have higher *Prdm16* than young males (1.8 ± 0.3 AU; $p < .05$). CR

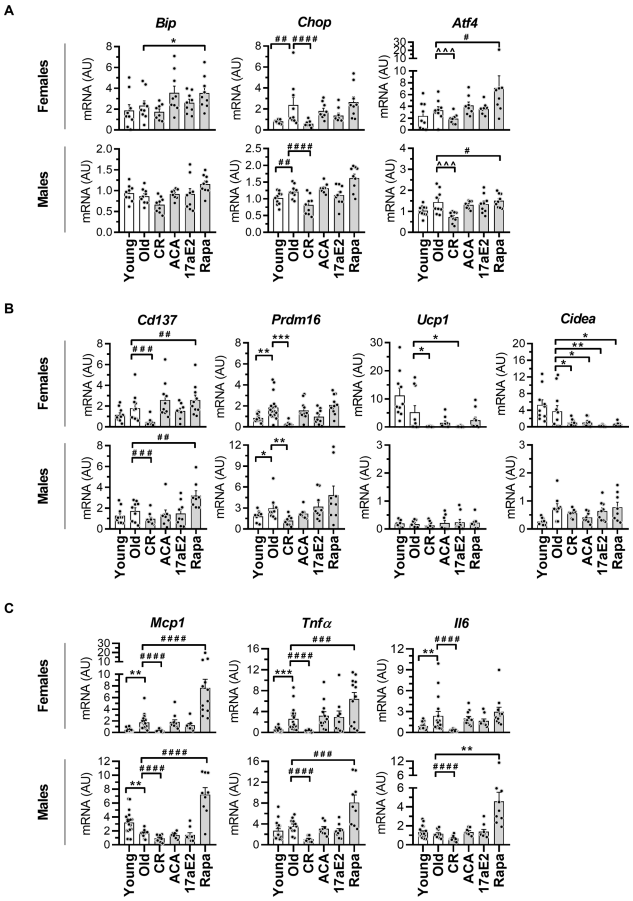

Figure 4. Expression of (**A**) endoplasmic reticulum (ER) stress genes (*Bip*, *Chop*, and *Atf4*); (**B**) brite markers (*Cd137*, *Prdm16*, *Ucp1*, and *Cidea*); and (**C**) proinflammatory chemokine and cytokines (*Mcp1*, *Tnfα*, and *Il6*) in gonadal white adipose tissue (gWAT). Error bars are SEM. Two-way analysis of variance (ANOVA), Sidak's multiple comparison's post hoc test ($*p < .05$, $**p < .01$, $***p < .001$, $****p < .0001$). If no sex effect was significant, sexes were pooled. Student's unpaired *T*-test ($\hat{}p < .05$, $\hat{}\hat{}p < .01$, $\hat{}\hat{}\hat{}p < .001$, $\hat{}\hat{}\hat{}\hat{}p < .0001$) or by Mann–Whitney if normality test failed ($^{\#}p < .05$, $^{\#\#}p < .01$, $^{\#\#\#}p < .001$, $^{\#\#\#\#}p < .0001$). n = 9–19 per group and sex and each sample was normalized to *Gapdh*.

decreases *Prdm16* in females (CR: 0.3 ± 0.1 AU, old: 1.9 ± 0.3 AU; $p < .001$) and males (CR: 1.2 ± 0.2 AU, old: 3.0 ± 0.2; $p < .01$). In males, there were no significant changes in *Ucp1* and *Cidea* expression in gWAT. In females, compared to old controls' expression of *Ucp1* (5.2 ± 2.4 AU) and *Cidea* (3.7 ± 1.4 AU), CR decreases *Ucp1* (0.2 ± 0.1 AU; $p < .05$) and *Cidea* (1.0 ± 0.2 AU; $p < .05$) expression. Interestingly, 17aE2-treated females similarly have significant decreases in *Ucp1* (0.17 ± 0.1 AU; $p < .05$) and *Cidea* (0.2 ± 0.1 AU; $p < .01$). ACA-treated females also have a significant decrease in *Cidea* (1.0 ± 0.3 AU; $p < .05$). The ITP drugs we tested appear to moderately affect a few of these thermogenic markers in gWAT at basal states (not cold challenged).

We measure proinflammatory chemo- and cytokine mRNA to assess adipose tissue inflammation in the HET3 mice (Figure 4C). Consistent with literature and the trends in our M1:M2 macrophage data, old female mice have increased adipose tissue inflammation compared to young controls. Old females express significantly higher *Mcp1* (1.7 ± 0.3 AU), *Tnfa* (2.6 ± 0.6 AU), and *Il6* (2.4 ± 0.6 AU) than young females (*Mcp1* 0.5 ± 0.1 AU, $p < .01$; *Tnfa* 0.6 ± 0.1 AU, $p <$

.001; *Il6* 0.9 ± 0.1 AU, $p < .01$). In contrast, young males (3.2 ± 0.4 AU) express higher *Mcp1* than old controls (1.7 ± 0.2 AU, $p < .01$). In congruence with our M1:M2 macrophage data, CR decreases and Rapa increases adipose tissue inflammation in old mice of both sexes (Figure 4C). CR mice express significantly decreased *Mcp1* (0.7 ± 0.1 AU), *Tnfa* (0.8 ± 0.1 AU), and *Il6* (0.5 ± 0.1 AU) compared to old controls (*Mcp1* 1.7 ± 0.2 AU, $p < .0001$; *Tnfa* 3.0 ± 0.4 AU, $p < .0001$; *Il6* 1.9 ± 0.4 AU, $p < .0001$). As expected from the significant increase of M1 ATMs in Rapa mice (Figure 3C), Rapa mice of both sexes also express significantly increased *Mcp1* (7.5 ± 0.9 AU) and *Tnfa* (0.8 ± 0.1 AU) compared to old controls (*Mcp1* 1.7 ± 0.2 AU, $p < .0001$; *Tnfa* 3.0 ± 0.4 AU, $p < .001$). In addition, Rapa males (4.6 ± 1.0 AU) express higher *Il6* than old males (1.2 ± 0.1 AU, $p < .01$).

Accumulation of Senescent Cells in iWAT

Senescent cells accumulate in aging adipose tissue, particularly in the iWAT, and they are thought to play a role in determining life span and healthspan (27,28). We measured *p16*, *p21*, and *p53* in the iWATs of HET3 mice (Figure 5) to assess if there is an effect of age on the accumulation of these senescent cells in these genetically heterogeneous mice. Both p16 and p21 are cell cycle inhibitors, and p53 is a primary tumor-suppressor pathway; these are important for the regulation of certain senescent states of cells (58–61). Consistent with literature (27,28,62), we observe an age-associated increase on senescent cell marker expression in iWAT of females (Figure 5). Old female mice have age-dependent increases of *p16* (young: 0.5 ± 0.1 AU, old: 2.5 ± 0.2 AU; $p < .0001$) and *p53* (young: 1.2 ± 0.2 AU, old: 2.2 ± 0.2 AU; $p < .0001$). Both old females and males (2.3 ± 0.4 AU) have an age-dependent increase of *p21* when compared to young controls (1.3 ± 0.1 AU; $p < .05$). CR female mice (0.5 ± 0.1 AU) have significantly decreased *p16* compared to old females ($p < .0001$), and CR females also have decreased *p53* (CR: 0.6 ± 0.2 AU, old: 2.2 ± 0.2 AU; $p < .0001$), and CR mice of both sexes (0.7 ± 0.1 AU) also have decreased *p21* compared to old controls (2.3 ± 0.4 AU; $p < .0001$) (Figure 5).

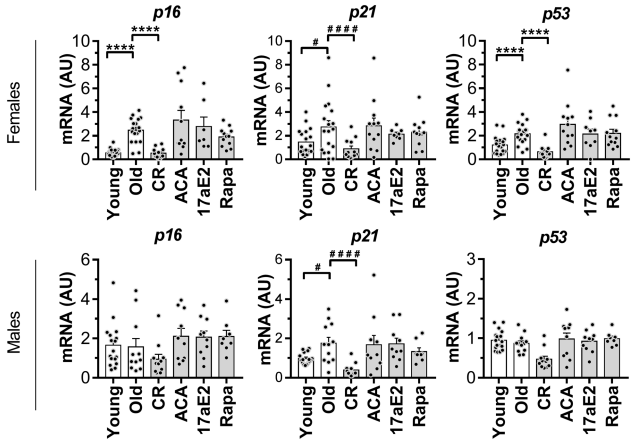

Figure 5. Effect of aging on inguinal white adipose tissue (iWAT) accumulation of senescent cells. Expression of senescence marker genes (*p16, p21,* and *p53*) in iWAT of HET3 mice. $n = 9–19$ per group per sex. Each sample was normalized to *Gapdh*. Error bars are SEM. Two-way analysis of variance (ANOVA), Sidak's multiple comparison's post hoc test (*$p < .05$, **$p < .01$, ***$p < .001$, ****$p < .0001$). If no sex effect was significant, sexes were pooled for analyses with either Student's unpaired *T*-test (^$p < .05$, ^^$p < .01$, ^^^$p < .001$, ^^^^$p < .0001$) or by Mann–Whitney if normality test failed (#$p < .05$, ##$p < .01$, ###$p < .001$, ####$p < .0001$).

Discussion

The ITP within the NIA is designed to identify treatments with the potential of life-span extension and delaying disease and dysfunction in mice. The three drugs we elected to test in this study, Rapa, ACA, and 17aE2, have all been shown to extend life span in mice. ACA and 17aE2 primarily benefit males, whereas Rapa extends life span in both sexes. These three drugs have been shown to affect a multitude of health outcomes in HET3 mice (39,40,42,43,45,63–65). However, the underlying mechanisms and organ-specific effects remain to be fully explored. How ITP drugs influence the aging processes and whether the different drugs influence life span through the same or different mechanisms are unclear.

CR is the classic approach that increases life span in healthy mice and has been regarded as the standard intervention for mammalian life-span extension. CR increases life span of HET3 mice by 32%–47% (44). Though not sufficient to completely explain CR-associated life-span extension, it has been posited that CR may influence life span through the loss of fat mass (30). Of note, the three ITP drugs we tested, Rapa, ACA, and 17aE2, have been associated with different metabolic outcomes in HET3 mice (40,66). However, very little is known about the effects of these drugs on adipose tissue. Given the important role of adipose tissue inflammation on age-related diseases, we hypothesized that these drugs' effect on adipose tissue inflammation could be an important mechanism in life-span extension.

ATMs are the major contributors to inflammation and metabolic dysfunction in diet-induced obesity (67–69). In age-related adiposity and metabolic syndrome, gWAT undergoes phenotypic switching from anti-inflammatory "M2" toward proinflammatory "M1" macrophage polarization (23). Our current data suggest old control HET3 mice have the greatest variability in the macrophage subset proportions, and this may be a limitation for our interpretation on the effect of age and individual treatment effect on these immune phenotypes. In this study, both ACA and 17aE2 treatments cause a trend toward increased M2 polarization in old male mice, although the results do not reach statistical significance. This is consistent with studies that have shown improved metabolic responses in male HET3 mice treated with ACA and 17aE2 (66). In CR males, there is significantly greater M2 polarization than non-CR old males, and while this trend was also present in females, it did not reach statistical significance. When we assessed the gWAT for proinflammatory chemokine and cytokine mRNA expression, we observe that CR leads to uniformly decreased *Mcp1*, *Tnfα*, and *Il6* in both sexes. These findings align with the association of CR to improved metabolic responses (40). In contrast, long-term dietary Rapa fed to HET3 mice leads to significant M1 ATM polarization in the gWAT along with significant increases in mRNA of *Mcp1*, *Tnfα*, and *Il6*. We also observe that the increase in $CD45^+$ leukocytes in the adipose tissue of Rapa-treated mice is due to an increase in total macrophages ($CD45^+CD64^+$).

Chronic Rapa treatment has been shown to induce differential outcomes of metabolic function; this has been suggested to be a reflection of different factors used in studies such as genotype, dose, length, and method of administration (70). Rapa induces glucose intolerance in rats (71) and C57BL6/J mice (70,72), as well as young and old HET3 mice (39). Interestingly, in contrast to C57BL6/J mice, insulin sensitivity remains largely unaffected in both young and old HET3 mice (39). It has been demonstrated that in vitro Rapa treatment induces a switch from M2 to M1 polarization and nearly eliminates $CD206^+$ expression in primary human macrophages (73).

A study has previously shown that short-term (30 days, gavage at 2 mg/kg/d) Rapa in C57BL/6J male mice in conjunction with diet-induced obesity (30 days of 60% high fat diet) significantly increased M1 macrophage polarization. Furthermore, inflammatory cytokine expression in epididymal adipose tissue increased in the absence of Rapa-induced fat mass changes (74). Our data are consistent with this—Rapa treatment in HET3 mice of both sexes strongly polarizes ATMs toward M1, and this was accompanied by increased proinflammatory expression of *Mcp1*, *Tnfα*, and *Il6* in Rapa-treated animals. We crucially observe that both sexes exhibited an increase in adipose tissue inflammation despite the body mass differences between Rapa-treated female and male HET3 mice. This strongly suggests that these proinflammatory changes, which could be attributed to fat mass gain, are not solely dependent on the Rapa-associated fat mass increases observed in the females of this current study. Given the known association between the proinflammatory "M1" macrophage and insulin resistance in diet-induced obesity (75), these data suggest that both acute and chronic Rapa treatments promote adipose tissue inflammation in part through rapid and dramatic induction of M1 polarization in ATMs.

When we assayed WATs for ER stress response genes (*Bip*, *Chop*, *Atf4*), beige/browning markers (*Cd137*, *Prdm16*, *Ucp1*, *Cidea*), and senescent cell markers (*p16*, *p21*, *p53*), we find that the three ITP drugs we tested (Rapa, ACA, and 17aE2) did not substantially affect these aging adipose tissue phenotypes. As expected, CR mice show delay in the effects of normal aging on these markers in adipose tissue. We previously reported that old C57BL/6J male mice have increased gWAT ER stress responses when challenged with thapsigargin *ex vivo*, leading to enhanced release of proinflammatory cytokines and chemokines in SVF cells and ATMs. *In vivo*, we reduced the secretion of these proinflammatory factors from the gWAT SVF with a chemical chaperone (25,26). In the current study, we find that *Chop* mRNA levels are increased in old controls while CR mice have reduced *Chop* and *Atf4*. In contrast to the CR mice, Rapa-treated females have an increase in *Bip* and *Atf4* (in males as well) mRNA. While limited to only assessment of mRNA, our data suggest that the three ITP drugs we tested may not facilitate life-span extension through alterations on ER stress responses in aging adipose tissue. Additionally, while there are sex differences in gWAT browning and beiging marker expression of *Prdm16*, *Ucp1*, and *Cidea*, we did not detect a strong effect of age in the HET3 mice with exception to *Prdm16* in both sexes.

Senescent cells accumulate in the iWAT to what appears to be a greater extent than gWAT (27,28), and they are thought to increase with age and play a role in determining life span and healthspan. We find that consistent with published literature (27,28), we detected higher number of senescent cells *p16*, *p21*, or *p53* in old HET3 mice iWAT. Consistent with a study of 17aE2 effects on C57BL6/J epididymal adipose tissue (42), we found no changes to the senescent markers in male HET3 iWAT. As expected, CR mice of both sexes have significantly lower senescent cell accumulation in iWAT. While there is some evidence that Rapa can reduce or suppress senescence positivity in vitro with young (2–3 months) *Nrf2* KO mouse fibroblasts (76), none of the three ITP drugs we tested alter the mRNA expression of senescent markers in the HET3 mice. Due to tissue limitations in this study, we could not further explore the extent to which these drugs may have affected browning/beiging capacities, senescent cell burdens, and ER stress of these mice. Future studies should employ a secondary challenge such as cold exposure to fully assess brite effects, and β-galactosidase staining of whole WAT may better characterize these ITP drugs' effect on senescent cell burden.

An important limitation of our study is that we were only able to assay the old HET3 mice at the 22-month time point. Male HET3 mice are shorter lived than their female counterparts, and weight loss is often seen in male HET3 mice beginning at approximately 18 months of age (40,41,45). In contrast, old female HET3 mice often maintain weight until the final few weeks of life (40,41,45). Consistent with published data, we found that aging has an important effect on adipose tissue inflammation in HET3 females, and the changes in the old male mice were less pronounced. This difference between female and male data may therefore also reflect survival effects of the cohort. We mentioned that ACA-treated animals in this study do not appear to exhibit the weight loss induced by ACA in a previous study (42). This previous study reported mice pooled from three ITP sites, and also includes site-specific data. Importantly, HET3 mice housed at UM appear to generate slightly smaller animals compared to other two ITP sites. In conjunction with weight loss in males prior to death, any ACA-associated weight loss would be difficult to discern at the 22-month time point in this current study for males. In contrast, we did not expect ACA-treated females to exhibit no weight loss differences. Weight loss has been deemed an unlikely life-span mechanism of ACA (42), because females experience greater weight loss than males and yet ACA extends female life span by 5% and males by 20%. This sexual dimorphic response to ACA has been attributed to the male-specific improvements of glucose tolerance and hepatic mTORC2 activity that are either absent or minimal in females (66). While the ACA-associated weight loss remains unexplained, an interesting recent report (77) demonstrates that ACA acts in a diet-dependent manner to affect murine gut microbial community structure. The discrepancies in weight loss in these mice may possibly reflect differences in microbiota between the different housing facilities during the previous study. In this current study, we did not determine if microbiota-diet interactions may have affected the weight loss in these mice, but futures studies should take this into consideration for ACA and other ITP drugs that may affect microbiota or interact with diet as a mechanism of action.

In summary, we found that CR and Rapa treatments influence aging adipose tissue inflammation differently. These observations add support to the notion that CR and Rapa treatments confer life-span extension in distinct ways (40). Our data also show ACA and 17aE2 generally did not influence any aspects of adipose tissue biology that we examined. Overall, this study indicates that of the three ITP drugs examined, only Rapa treatment affects adipose tissue inflammation, possibly exacerbating it, in both sexes of HET3 mice. Additional studies will be needed to determine whether or not these Rapa-associated ATM changes directly contribute to life-span extension. Future studies of adipose tissue biology of aging should also take into account sex differences in age-related adiposity changes.

Supplementary Material

Supplementary data are available at *The Journals of Gerontology, Series A: Biological Sciences and Medical Sciences* online.

Funding

This work was supported by Glenn Foundation for Medical Research; the National Institutes of Health (NIH) grants AG022303 (R.A.M.), AG024824 (R.Y.); Research Training in Experimental Immunology Training Grant T32-AI007413 (T.M.); Career Training in the Biology of Aging Training Grant

T32-AG000114 (T.M.); and Geriatrics Research, Education and Clinical Care Center (GRECC) of the VA Ann Arbor Healthcare System (R.Y.). The content is solely the responsibility of the authors and does not necessarily represent the official views of the NIH.

Conflict of Interest

None reported.

References

1. Fagiolo U, Cossarizza A, Scala E, et al. Increased cytokine production in mononuclear cells of healthy elderly people. *Eur J Immunol*. 1993;23(9):2375–2378. doi:10.1002/eji.1830230950
2. Baggio G, Donazzan S, Monti D, et al. Lipoprotein(a) and lipoprotein profile in healthy centenarians: a reappraisal of vascular risk factors. *FASEB J*. 1998;12(6):433–437. doi:10.1096/fasebj.12.6.433
3. Bonafè M, Olivieri F, Cavallone L, et al. A gender-dependent genetic predisposition to produce high levels of IL-6 is detrimental for longevity. *Eur J Immunol*. 2001;31(8):2357–2361. doi:10.1002/1521-4141(200108)31:8<2357::AID-IMMU2357gt;3.0.CO;2-X
4. Coppola R, Mari D, Lattuada A, Franceschi C. Von Willebrand factor in Italian centenarians. *Haematologica*. 2003;88(1):39–43.
5. Zanni F, Vescovini R, Biasini C, et al. Marked increase with age of type 1 cytokines within memory and effector/cytotoxic $CD8^+$ T cells in humans: a contribution to understand the relationship between inflammation and immunosenescence. *Exp Gerontol*. 2003;38(9):981–987.
6. Franceschi C, Olivieri F, Marchegiani F, et al. Genes involved in immune response/inflammation, IGF1/insulin pathway and response to oxidative stress play a major role in the genetics of human longevity: the lesson of centenarians. *Mech Ageing Dev*. 2005;126:351–361. doi:10.1016/j.mad.2004.08.028
7. Wikby A, Nilsson BO, Forsey R, et al. The immune risk phenotype is associated with IL-6 in the terminal decline stage: findings from the Swedish NONA immune longitudinal study of very late life functioning. *Mech Ageing Dev*. 2006;127(8):695–704. doi:10.1016/j.mad.2006.04.003
8. Krabbe KS, Pedersen M, Bruunsgaard H. Inflammatory mediators in the elderly. *Exp Gerontol*. 2004;39(5):687–699. doi:10.1016/j.exger.2004.01.009
9. Howcroft TK, Campisi J, Louis GB, et al. The role of inflammation in age-related disease. *Aging (Albany NY)*. 2013;5(1):84–93. doi:10.18632/aging.100531
10. Franceschi C, Campisi J. Chronic inflammation (inflammaging) and its potential contribution to age-associated diseases. *J Gerontol A Biol Sci Med Sci*. 2014;69(Suppl. 1):S4–S9. doi:10.1093/gerona/glu057
11. Tchkonia T, Morbeck DE, Von Zglinicki T, et al. Fat tissue, aging, and cellular senescence. *Aging Cell*. 2010;9(5):667–684. doi:10.1111/j.1474-9726.2010.00608.x
12. Mau T, Yung R. Adipose tissue inflammation in aging. *Exp Gerontol*. 2018;105:27–31. doi:10.1016/j.exger.2017.10.014
13. Palmer AK, Kirkland JL. Aging and adipose tissue: potential interventions for diabetes and regenerative medicine. *Exp Gerontol*. 2016;86:97–105. doi:10.1016/j.exger.2016.02.013
14. Park SE, Park CY, Choi JM, et al. Depot-specific changes in fat metabolism with aging in a type 2 diabetic animal model. *PLoS One*. 2016;11(2):e0148141. doi:10.1371/journal.pone.0148141
15. Barzilai N, Rossetti L. Relationship between changes in body composition and insulin responsiveness in models of the aging rat. *Am J Physiol*. 1995;269(3 Pt 1):E591–E597. doi:10.1152/ajpendo.1995.269.3.E591
16. Guo SS, Zeller C, Chumlea WC, Siervogel RM. Aging, body composition, and lifestyle: the Fels Longitudinal Study. *Am J Clin Nutr*. 1999;70(3):405–411. doi:10.1093/ajcn/70.3.405
17. Kyle UG, Genton L, Hans D, Karsegard L, Slosman DO, Pichard C. Age-related differences in fat-free mass, skeletal muscle, body cell mass and fat mass between 18 and 94 years. *Eur J Clin Nutr*. 2001;55:663–672. doi:10.1038/sj.ejcn.1601198
18. Kuk JL, Saunders TJ, Davidson LE, Ross R. Age-related changes in total and regional fat distribution. *Ageing Res Rev*. 2009;8(4):339–348. doi:10.1016/j.arr.2009.06.001
19. Marcus RL, Addison O, Kidde JP, Dibble LE, Lastayo PC. Skeletal muscle fat infiltration: impact of age, inactivity, and exercise. *J Nutr Health Aging*. 2010;14(5):362–366.
20. Shimomura I, Hammer RE, Richardson JA, et al. Insulin resistance and diabetes mellitus in transgenic mice expressing nuclear SREBP-1c in adipose tissue: model for congenital generalized lipodystrophy. *Genes Dev*. 1998;12(20):3182–3194. doi:10.1101/gad.12.20.3182
21. Hamrick MW, Ding KH, Pennington C, et al. Age-related loss of muscle mass and bone strength in mice is associated with a decline in physical activity and serum leptin. *Bone*. 2006;39(4):845–853. doi:10.1016/j.bone.2006.04.011
22. Périè L, Parenté A, Baraige F, Magnol L, Blanquet V. Alterations in adiposity and glucose homeostasis in adult Gasp-1 overexpressing mice. *Cell Physiol Biochem*. 2018;44(5):1896–1911. doi:10.1159/000485878.
23. Lumeng CN, Liu J, Geletka L, et al. Aging is associated with an increase in T cells and inflammatory macrophages in visceral adipose tissue. *J Immunol*. 2011;187(12):6208–6216. doi:10.4049/jimmunol.1102188
24. Garg SK, Delaney C, Toubai T, et al. Aging is associated with increased regulatory T-cell function. *Aging Cell*. 2014;13(3):441–448. doi:10.1111/acel.12191
25. Ghosh AK, Garg SK, Mau T, O'Brien M, Liu J, Yung R. Elevated endoplasmic reticulum stress response contributes to adipose tissue inflammation in aging. *J Gerontol A Biol Sci Med Sci*. 2015;70(11):1320–1329. doi:10.1093/gerona/glu186
26. Ghosh AK, Mau T, O'Brien M, Garg S, Yung R. Impaired autophagy activity is linked to elevated ER-stress and inflammation in aging adipose tissue. *Aging (Albany NY)*. 2016;8(10):2525–2537. doi:10.18632/aging.101083
27. Baker DJ, Wijshake T, Tchkonia T, et al. Clearance of p16Ink4a-positive senescent cells delays ageing-associated disorders. *Nature*. 2011;479(7372):232–236. doi:10.1038/nature10600
28. Baker DJ, Childs BG, Durik M, et al. Naturally occurring p16(Ink4a)-positive cells shorten healthy lifespan. *Nature*. 2016;530(7589):184–189. doi:10.1038/nature16932
29. Huffman DM, Barzilai N. Contribution of adipose tissue to health span and longevity. *Interdiscip Top Gerontol*. 2010;37:1–19. doi:10.1159/000319991
30. Barzilai N, Gupta G. Revisiting the role of fat mass in the life extension induced by caloric restriction. *J Gerontol A Biol Sci Med Sci*. 1999;54(3):B89–96; discussion B97. doi:10.1093/gerona/54.3.b89
31. Gabriely I, Ma XH, Yang XM, et al. Removal of visceral fat prevents insulin resistance and glucose intolerance of aging: an adipokine-mediated process? *Diabetes*. 2002;51(10):2951–2958. doi:10.2337/diabetes.51.10.2951
32. Blüher M, Kahn BB, Kahn CR. Extended longevity in mice lacking the insulin receptor in adipose tissue. *Science*. 2003;299(5606):572–574. doi:10.1126/science.1078223
33. Stout MB, Tchkonia T, Pirtskhalava T, et al. Growth hormone action predicts age-related white adipose tissue dysfunction and senescent cell burden in mice. *Aging (Albany NY)*. 2014;6(7):575–586. doi:10.18632/aging.100681
34. Stout MB, Steyn FJ, Jurczak MJ, et al. 17α-Estradiol alleviates age-related metabolic and inflammatory dysfunction in male mice without inducing feminization. *J Gerontol A Biol Sci Med Sci*. 2017;72(1):3–15. doi:10.1093/gerona/glv309
35. Giannakou ME, Goss M, Jünger MA, Hafen E, Leevers SJ, Partridge L. Long-lived *Drosophila* with overexpressed dFOXO in adult fat body. *Science*. 2004;305(5682):361. doi:10.1126/science.1098219
36. Libina N, Berman JR, Kenyon C. Tissue-specific activities of *C. elegans* DAF-16 in the regulation of lifespan. *Cell*. 2003;115(4):489–502. doi:10.1016/s0092-8674(03)00889-4
37. Harrison DE, Strong R, Sharp ZD, et al. Rapamycin fed late in life extends lifespan in genetically heterogeneous mice. *Nature*. 2009;460(7253):392–395. doi:10.1038/nature08221

38. Wilkinson JE, Burmeister L, Brooks SV, et al. Rapamycin slows aging in mice. *Aging Cell*. 2012;11(4):675–682. doi:10.1111/j.1474-9726.2012.00832.x
39. Lamming DW, Ye L, Astle CM, Baur JA, Sabatini DM, Harrison DE. Young and old genetically heterogeneous HET3 mice on a rapamycin diet are glucose intolerant but insulin sensitive. *Aging Cell*. 2013;12(4):712–718. doi:10.1111/acel.12097
40. Miller RA, Harrison DE, Astle CM, et al. Rapamycin-mediated lifespan increase in mice is dose and sex dependent and metabolically distinct from dietary restriction. *Aging Cell*. 2014;13(3):468–477. doi:10.1111/acel.12194
41. Miller RA, Harrison DE, Astle CM, et al. An aging Interventions Testing Program: study design and interim report. *Aging Cell*. 2007;6(4):565–575. doi:10.1111/j.1474-9726.2007.00311.x
42. Harrison DE, Strong R, Allison DB, et al. Acarbose, 17-α-estradiol, and nordihydroguaiaretic acid extend mouse lifespan preferentially in males. *Aging Cell*. 2014;13(2):273–282. doi:10.1111/acel.12170
43. Zaseck LW, Miller RA, Brooks SV. Rapamycin attenuates age-associated changes in tibialis anterior tendon viscoelastic properties. *J Gerontol A Biol Sci Med Sci*. 2016;71(7):858–865. doi:10.1093/gerona/glv307
44. Flurkey K, Astle CM, Harrison DE. Life extension by diet restriction and N-acetyl-L-cysteine in genetically heterogeneous mice. *J Gerontol A Biol Sci Med Sci*. 2010;65(12):1275–1284. doi:10.1093/gerona/glq155
45. Miller RA, Harrison DE, Astle CM, et al. Rapamycin, but not resveratrol or simvastatin, extends life span of genetically heterogeneous mice. *J Gerontol A Biol Sci Med Sci*. 2011;66(2):191–201. doi:10.1093/gerona/glq178
46. Nadon NL, Strong R, Miller RA, Harrison DE. NIA Interventions Testing Program: investigating putative aging intervention agents in a genetically heterogeneous mouse model. *EBioMedicine*. 2017;21:3–4. doi:10.1016/j.ebiom.2016.11.038
47. Miller RA, Burke D, Nadon N. Announcement : four-way cross mouse stocks: a new, genetically heterogeneous resource for aging research. *J Gerontol Biol Sci*. 1999;54(8):1999–2001.
48. Sun L, Sadighi Akha AA, Miller RA, Harper JM. Life-span extension in mice by preweaning food restriction and by methionine restriction in middle age. *Journals Gerontol A: Biol Sci Med Sci*. 2009;64(7):711–722. doi:10.1093/gerona/glp051
49. Pascot A, Lemieux S, Prud'homme D, et al. Age-related increase in visceral adipose tissue and the metabolic risk profile of premenopausal women. *Diabetes Care*. 1999;22(9):1471–1478.
50. Tardif N, Salles J, Guillet C, et al. Muscle ectopic fat deposition contributes to anabolic resistance in obese sarcopenic old rats through eIF2α activation. *Aging Cell*. 2014;13(6):1001–1011. doi:10.1111/acel.12263
51. Wu D, Ren Z, Pae M, et al. Aging up-regulates expression of inflammatory mediators in mouse adipose tissue. *J Immunol*. 2007;179(7):4829–4839. doi:10.4049/jimmunol.179.7.4829
52. Gautier EL, Shay T, Miller J, et al.; Immunological Genome Consortium. Gene-expression profiles and transcriptional regulatory pathways that underlie the identity and diversity of mouse tissue macrophages. *Nat Immunol*. 2012;13(11):1118–1128. doi:10.1038/ni.2419
53. Cho KW, Zamarron BF, Muir LA, et al. Adipose tissue dendritic cells are independent contributors to obesity-induced inflammation and insulin resistance. *J Immunol*. 2016;197(9):3650–3661. doi:10.4049/jimmunol.1600820
54. Yoneshiro T, Aita S, Matsushita M, et al. Age-related decrease in cold-activated brown adipose tissue and accumulation of body fat in healthy humans. *Obesity (Silver Spring)*. 2011;19(9):1755–1760. doi:10.1038/oby.2011.125
55. Rogers NH, Landa A, Park S, Smith RG. Aging leads to a programmed loss of brown adipocytes in murine subcutaneous white adipose tissue. *Aging Cell*. 2012;11(6):1074–1083. doi:10.1111/acel.12010
56. Wu J, Boström P, Sparks LM, et al. Beige adipocytes are a distinct type of thermogenic fat cell in mouse and human. *Cell*. 2012;150(2):366–376. doi:10.1016/j.cell.2012.05.016
57. Seale P, Conroe HM, Estall J, et al. Prdm16 determines the thermogenic program of subcutaneous white adipose tissue in mice. *J Clin Invest*. 2011;121(1):96–105. doi:10.1172/JCI44271
58. Brown JP, Wei W, Sedivy JM. Bypass of senescence after disruption of p21CIP1/WAF1 gene in normal diploid human fibroblasts. *Science*. 1997;277(5327):831–834. doi:10.1126/science.277.5327.831
59. Gire V, Wynford-Thomas D. Reinitiation of DNA synthesis and cell division in senescent human fibroblasts by microinjection of anti-p53 antibodies. *Mol Cell Biol*. 1998;18(3):1611–1621. doi:10.1128/mcb.18.3.1611
60. Campisi J. Senescent cells, tumor suppression, and organismal aging: good citizens, bad neighbors. *Cell*. 2005;120(4):513–522. doi:10.1016/j.cell.2005.02.003
61. Di Micco R, Fumagalli M, Cicalese A, et al. Oncogene-induced senescence is a DNA damage response triggered by DNA hyper-replication. *Nature*. 2006;444(7119):638–642. doi:10.1038/nature05327
62. Krishnamurthy J, Torrice C, Ramsey MR, et al. Ink4a/Arf expression is a biomarker of aging. *J Clin Invest*. 2004;114(9):1299–1307. doi:10.1172/JCI200422475
63. Strong R, Miller RA, Antebi A, et al. Longer lifespan in male mice treated with a weakly estrogenic agonist, an antioxidant, an α-glucosidase inhibitor or a Nrf2-inducer. *Aging Cell*. 2016;15(5):872–884. doi:10.1111/acel.12496
64. Strong R, Miller RA, Astle CM, et al. Nordihydroguaiaretic acid and aspirin increase lifespan of genetically heterogeneous male mice. *Aging Cell*. 2008;7(5):641–650. doi:10.1111/j.1474-9726.2008.00414.x
65. Garratt M, Nakagawa S, Simons MJ. Comparative idiosyncrasies in life extension by reduced mTOR signalling and its distinctiveness from dietary restriction. *Aging Cell*. 2016;15(4):737–743. doi:10.1111/acel.12489
66. Garratt M, Bower B, Garcia GG, Miller RA. Sex differences in lifespan extension with acarbose and 17-α estradiol: gonadal hormones underlie male-specific improvements in glucose tolerance and mTORC2 signaling. *Aging Cell*. 2017;16(6):1256–1266. doi:10.1111/acel.12656
67. Hotamisligil GS, Shargill NS, Spiegelman BM. Adipose expression of tumor necrosis factor-alpha: direct role in obesity-linked insulin resistance. *Science*. 1993;259(5091):87–91. doi:10.1126/science.7678183
68. Weisberg SP, McCann D, Desai M, Rosenbaum M, Leibel RL, Ferrante AW Jr. Obesity is associated with macrophage accumulation in adipose tissue. *J Clin Invest*. 2003;112(12):1796–1808. doi:10.1172/JCI19246
69. Lumeng CN, Bodzin JL, Saltiel AR. Obesity induces a phenotypic switch in adipose tissue macrophage polarization. *J Clin Invest*. 2007;117(1):175–184. doi:10.1172/JCI29881
70. Lamming DW, Ye L, Katajisto P, et al. Rapamycin-induced insulin resistance is mediated by mTORC2 loss and uncoupled from longevity. *Science*. 2012;335(6076):1638–1643. doi:10.1126/science.1215135
71. Houde VP, Brûlé S, Festuccia WT, et al. Chronic rapamycin treatment causes glucose intolerance and hyperlipidemia by upregulating hepatic gluconeogenesis and impairing lipid deposition in adipose tissue. *Diabetes*. 2010;59(6):1338–1348. doi:10.2337/db09-1324
72. Fok WC, Zhang Y, Salmon AB, et al. Short-term treatment with rapamycin and dietary restriction have overlapping and distinctive effects in young mice. *J Gerontol A Biol Sci Med Sci*. 2013;68(2):108–116. doi:10.1093/gerona/gls127
73. Mercalli A, Calavita I, Dugnani E, et al. Rapamycin unbalances the polarization of human macrophages to M1. *Immunology*. 2013;140(2):179–190. doi:10.1111/imm.12126
74. Paschoal VA, Amano MT, Belchior T, et al. mTORC1 inhibition with rapamycin exacerbates adipose tissue inflammation in obese mice and dissociates macrophage phenotype from function. *Immunobiology*. 2017;222(2):261–271. doi:10.1016/j.imbio.2016.09.014.
75. Han MS, Jung DY, Morel C, et al. JNK expression by macrophages promotes obesity-induced insulin resistance and inflammation. *Science*. 2013;339(6116):218–222. doi:10.1126/science.1227568.
76. Wang R, Yu Z, Sunchu B, et al. Rapamycin inhibits the secretory phenotype of senescent cells by a Nrf2-independent mechanism. *Aging Cell*. 2017. doi:10.1111/acel.12587.
77. Baxter NT, Lesniak NA, Sinani H, Schloss PD, Koropatkin NM. The glucoamylase inhibitor acarbose has a diet-dependent and reversible effect on the murine gut microbiome. *mSphere*. 2019;4(1):e00528–18. doi:10.1128/mSphere.00528-18..